Inverse Problems **16** (2000) 1–12. Printed in the UK PII: S0266-5611(00)10176-5

Raman solitons in transient SRS

M Boiti†‡, J-G Caputo†, J Leon† and F Pempinelli†‡

† Physique Mathématique et Théorique, CNRS-UMR5825, Université Montpellier 2, 34095 Montpellier, France

‡ Dipartimento di Fisica dell' Università, Lecce, Italy

Received 8 December 1999

Abstract. We report on the observation of Raman solitons on numerical simulations of transient stimulated Raman scattering with small group-velocity dispersion. The theory proceeds with the inverse scattering transform (IST) for initial boundary-value problems and it is shown that the explicit theoretical solution obtained by IST for a semi-infinite medium fits strikingly well the numerical solution for a finite medium. We are able to explain this in terms of the rapid decrease of the medium dynamical variable (the potential of the scattering theory). The spectral transform reflection coefficient can be computed directly from the values of the input and output fields and this allows one to see the generation of the Raman solitons from the numerical solution. We confirm the presence of these nonlinear modes in the medium dynamical variable by the use of a discrete spectral analysis.

1. Introduction

Stimulated Raman scattering (SRS) is a three-wave interaction process with extremely wide application in physics, especially in nonlinear optics [1, 2]. This essentially nonlinear phenomenon couples two electromagnetic waves (pump and Stokes waves) to a two-level medium and is described by a simple system of partial differential equations [3].

Such a system applies to different physical situations, depending on a phenomenological damping factor chosen to match the observed Raman linewidth. For instance, the steady state regime occurs when one neglects dynamical effects on the medium. Then the system becomes explicitly solvable in terms of the intensities and the result fits well the situation of strong damping and long pulses, such as in fibre guides [4]. Alternatively, when the dynamical effects and damping are of the same order, very interesting phase effects have been discovered [5]. These have been interpreted as the manifestation of solitons which, in the spectral transform scheme, would be related to discrete eigenvalues. Instead they are related to the continuous spectrum (they are not solitons) and have been given the name *Raman spikes* [6]. Therefore, the question relating to the observation of Raman solitons has remained open since the original work [3] performed in 1975.

When the damping term is much smaller than the dynamical response of the medium, and can be neglected, the regime is called hyper-transient and applies to short-duration pulses. Here the system possesses a Lax pair [3, 7, 8] and can be treated by means of the inverse scattering transform (IST) generalized to boundary-value problems [9, 10]. The observation of the Raman soliton is an interesting open problem, especially since the boundary-value problem for TSRS has been completely solved on the finite interval in [11] with the essential result that,

0266-5611/00/000001+12$30.00 © 2000 IOP Publishing Ltd

Processing IP/110176/PAP
Focal Image
Printed: 4/02/2000
To author
.....

CRC data
File name IP .TEX First page
Date req. Last page
Issue no. Total pages

as expected from the works [12–14], the field $q(x, t)$ universally evolves toward the self-similar solution.

The commonly used transient stimulated Raman scattering (TSRS) model is obtained as a three-wave interaction process where the group velocities of the three fields involved are considered equal. As shown in [15], this assumption is an asymptotic limit and consequently the group-velocity dispersion (GVD) has to be taken into account (through the spectral extension of the input laser fields), leading to a modified SRS system (see (2.2) below). The main consequence of this fact is that Raman solitons (discrete eigenvalues in the nonlinear Fourier spectrum) are effectively generated by SRS in the medium [15].

The aim of this paper is to show that Raman solitons are indeed created in a finite-length medium and that their generation is accompanied with poles in the nonlinear Fourier spectrum (spectral transform). We follow the model derived and solved in [15] and establish the following results.

(1) Based on the assumption of a semi-infinite medium, IST gives an explicit solution† which will be shown to be an excellent approximation of the finite-medium case. We explain this in terms of the fast decay of the *potential* $q(x, t)$ for large x. Such is not the case in the zero-GVD case for which $q(x, t)$ decreases as $x^{-3/4}$, which is typical of the self-similar solution [11, 12].
(2) The reflection coefficient ρ of the spectral transform (or nonlinear Fourier spectrum) is expressed in terms of the input and output field envelopes, allowing us to check the appearance of Raman solitons (the real-valued single poles of ρ) on the numerical solutions. This also provides a means to observe the generation of Raman solitons in experimental data.
(3) A recursion formula for computing the spectral transform of a finite set of data has been recently proposed [16]. We have implemented this *discrete spectral transform* and confirmed the creation of these Raman solitons in a simulation on a finite length. A remarkable feature here is that the numerical spectral transform can be quite easily implemented, its computation is faster, and it provides more information than a conventional Fourier transform.

After presenting the model in section 2, we report on the numerical observation of the Raman solitons in section 3. Section 4 explains this by an analysis of the medium dynamical variable.

2. The model

We present here the extension of the SRS model of [3] to the case where the dispersion of the group velocity is not neglected. We consider the classical model as in [2], well adapted to molecular Raman scattering, and for which the medium is schematically represented by a collection X of harmonic oscillators coupled to the electric field $\vec{E}$ through the polarizability of the medium.

2.1. Basic equations

When the polarizability depends on the frequency of the applied field, the group velocity of the electromagnetic waves becomes frequency dependent. While a very small GVD has no

† The solution is not explicit for the finite-length case: both the results of [15] and [11] give the answer by solving a system of Cauchy–Green integral equations.

consequence on the evolution of the amplitude, it has nontrivial effects on the phase dynamics. In this context, it has been proved in [15], using *multiscale analysis*, that for the electric field

$$E(x,t') = \mathrm{e}^{\mathrm{i}(k_1 x-\omega_1 t')}\int \mathrm{d}k a(k,x,t)\mathrm{e}^{-\mathrm{i}kx} + \mathrm{e}^{\mathrm{i}(k_2 x-\omega_2 t')}\sqrt{\frac{\omega_2}{\omega_1}}\int \mathrm{d}k b(k,x,t)\mathrm{e}^{\mathrm{i}kx} + \text{c.c.} \tag{2.1}$$

and medium dynamical variable $q(x,t)\mathrm{e}^{\mathrm{i}(Kx-\Omega t')} + \text{c.c.}$, where $\omega_1 - \omega_2 = \Omega$ and $k_1 - k_2 = K$, the resulting model of transient SRS can be written in the *retarded time* $t = t' - x/v$

$$\begin{aligned} &\partial_x a = qb\mathrm{e}^{2\mathrm{i}kx}, \qquad \partial_x b = -\bar{q}a\mathrm{e}^{-2\mathrm{i}kx}, \\ &\partial_t q = -g\int \mathrm{d}k a\bar{b}\mathrm{e}^{-2\mathrm{i}kx}, \end{aligned} \tag{2.2}$$

where in all cases the overbar stands for the complex conjugate. Note the conservation (x-independence) of the flux density $|a|^2 + |b|^2$.

The above model differs from the usual SRS system, corresponding to the zero-GVD case

$$\partial_x a = q_0 b, \qquad \partial_x b = -\bar{q}_0 a, \qquad \partial_t q_0 = -ga\bar{b}, \tag{2.3}$$

by the presence of the integral over all possible realizations of the phase mismatch k.

2.2. Boundary-value problem

The question of interest is the time evolution of a couple (a, b) of pump and Stokes pulses of time duration T sent into a medium of length ℓ. Hence the domain of integration is

$$x \in [0,\ell], \qquad t \in [0,T]. \tag{2.4}$$

and it is necessary to prescribe the values of the fields on the two boundaries $t = 0$ and $x = 0$. The medium is initially ($t = 0$) at rest (all molecules in the fundamental state), hence the initial datum for the field q is

$$q(x,0) = 0, \tag{2.5}$$

independently of the reference frame†.

The input ($x = 0$) light pulses are arbitrary functions of time t with a given spectral distribution around $k = 0$, namely

$$a(k,0,t) = A(k,t), \qquad b(k,0,t) = B(k,t). \tag{2.6}$$

We shall be working here with the representative example treated in [15] which consists of assuming a common spectral lineshape for A and B as a normalized Lorentzian lineshape for the intensities. More precisely we set

$$|A(k,t)|^2 = |A_0(t)|^2\frac{1}{\pi}\frac{\kappa}{k^2+\kappa^2}, \qquad |B(k,t)|^2 = |B_0(t)|^2\frac{1}{\pi}\frac{\kappa}{k^2+\kappa^2}, \tag{2.7}$$

where the input pulse profiles $A_0(t)$ and $B_0(t)$ are arbitrary.

It is useful also to understand the scale invariance of the SRS system, including its boundary values. By a simple change of variables it can be easily shown that the system (2.2) (characterized by the parameters g and ℓ) *together with* the input boundary values (2.6), (2.7) (characterized by the parameter κ) bears the scale invariance

$$\ell \to \alpha\ell, \qquad g \to g/\alpha, \qquad \kappa \to \kappa/\alpha. \tag{2.8}$$

This invariance has been checked on numerical simulations as a way to test the code accuracy, and it works so well that we have obtained indiscernible plots. Note 1

† Note that a *prepared* medium would correspond to a state q given at *physical time* zero, that is on the characteristic $t = -x/v$.

3. Laser fields

In what follows we describe the IST solution of the boundary-value problem (2.6) for the system (2.2) using the results of [15], and compare it with the direct numerical solution in the finite-length case.

3.1. Sketch of the direct problem

The direct problem consists of defining the spectral transform from the data of the *potential* $q(x,t)$ and the boundary values $A(k,t)$ and $B(k,t)$ (as time t appears everywhere as an external parameter, we shall omit it here). This is carried out by defining the following Jost solutions (for $k \in \mathbb{R}$):

$$\begin{aligned} \varphi(k,x) &= 1 - \int_0^x \mathrm{d}\xi\, q(\xi)\phi(k,\xi), \\ \phi(k,x) &= \int_0^x \mathrm{d}\xi\, \overline{q}(\xi)\varphi(k,\xi)\mathrm{e}^{2\mathrm{i}k(x-\xi)}, \end{aligned} \tag{3.1}$$

which are both entire functions of k vanishing as $k \to \infty$ in the upper half-plane†.

These two functions then allow one to define the *reflection coefficient* $\rho(k)$ and the *transmission coefficient* $\tau(k)$ by taking the limit $x \to \infty$ of φ and $\overline{\phi}\mathrm{e}^{2\mathrm{i}kx}$ for $k \in \mathbb{R}$, namely

$$\frac{1}{\tau} = 1 - \int_0^\infty \mathrm{d}\xi\, q(\xi)\phi(k,\xi), \qquad \frac{\rho}{\tau} = -\int_0^\infty \mathrm{d}\xi\, q(\xi)\overline{\varphi}(k,\xi)\mathrm{e}^{2\mathrm{i}k\xi}. \tag{3.2}$$

The coefficient $1/\tau$ is clearly an entire function of k and one can show [15] that the reflection coefficient $\rho(k)$ is meromorphic in the upper half-plane with a finite number of single poles related to the solitonic part of the solution q. We also have the following *unitarity* relation for $k \in \mathbb{R}$:

$$|\rho|^2 = 1 + |\tau|^2. \tag{3.3}$$

It is easy to finally prove that the vectors $(\varphi, -\phi\mathrm{e}^{-2\mathrm{i}kx})$ and $(\overline{\phi}\mathrm{e}^{2\mathrm{i}kx}, \overline{\varphi})$ solve the same differential equation as the vector (a,b) in (2.2). Then, by comparing their values in $x = 0$, we readily obtain from (2.6):

$$a = A\varphi + B\overline{\phi}\mathrm{e}^{2\mathrm{i}kx}, \qquad b = B\overline{\varphi} - A\phi\mathrm{e}^{-2\mathrm{i}kx}. \tag{3.4}$$

3.2. Output pump pulse

From (3.2)–(3.4), the output $|a(k,\ell,t)|^2$ is explicitly given for $\ell \to \infty$ by the expression

$$|a(k,\infty,t)|^2 = \frac{1}{1+|\rho|^2}|A - \rho B|^2, \tag{3.5}$$

where A and B are the input data defined in (2.6).

The main result of [15] is that the function $\rho(k,t)$ is obtained by solving the following Riccati time evolution:

$$\rho_t = -\rho^2 \mathcal{C}_k^+[m^*] - 2\rho\mathcal{C}_k^+[\phi] - \mathcal{C}_k^+[m], \qquad \rho(k,0) = 0, \tag{3.6}$$

where the functions $m(k,t)$ and $\phi(k,t)$ are given from the input data by

$$m = \frac{\mathrm{i}\pi}{2} g A B^*, \qquad \phi = \frac{\mathrm{i}\pi}{4} g(|A|^2 - |B|^2), \tag{3.7}$$

† The relation with notations of [15] is $\varphi(k) = \varphi_{11}^+(k) = \overline{\varphi_{22}^-}(\bar{k})$, $\phi(k) = -\varphi_{21}^+(k) = \overline{\varphi_{12}^-}(\bar{k})$.

and where $\mathcal{C}_k^+$ denotes the following Cauchy integral:

$$\mathcal{C}_k^+[f] = \frac{1}{\pi}\int_{-\infty}^{+\infty} \frac{\mathrm{d}\zeta}{\zeta - (k + \mathrm{i}0)} f(\zeta). \tag{3.8}$$

Consequently, for given inputs $A(k,t)$ and $B(k,t)$, (3.5) gives the explicit asymptotic output pump intensity from the solution of the evolution (3.6). It is worth noting that, at any given time, ρ possesses possibly a finite number of simple poles whose time evolution is given by the nonlinearity of the Riccati equation.

For practical reasons, in (2.6) we choose the Stokes wave input seed as a portion $\mathrm{e}^{-\gamma}$ of the pump wave, namely

$$B_0(t) = A_0(t)\mathrm{e}^{-\gamma}. \tag{3.9}$$

In this case the evolution (3.6) can be explicitly solved [15]:

$$\rho(k,t) = \frac{\sinh\delta(k,t)}{\cosh(\delta(k,t) - \gamma)}, \tag{3.10}$$

$$\delta(k,t) = \frac{\mathrm{i}T(t)}{k + \mathrm{i}\kappa}, \qquad T(t) = \tfrac{1}{4}g(1 + \mathrm{e}^{-2\gamma})\int_0^t \mathrm{d}\tau |A_0(\tau)|^2. \tag{3.11}$$

3.3. Numerical solution of finite-length TSRS

Our purpose is to understand how the above IST solution can be used to model the solution of the SRS system (2.2) on a finite length. This can be done first in a qualitative way by writing the solution of (2.2) with boundary values (2.6) as the equivalent integral form

$$\begin{pmatrix} a(k,x,t) \\ b(k,x,t) \end{pmatrix} = \begin{pmatrix} A(k,t) \\ B(k,t) \end{pmatrix} + \int_0^x \mathrm{d}\xi \begin{pmatrix} q(\xi,t)b(k,\xi,t)\mathrm{e}^{2\mathrm{i}k\xi} \\ -\overline{q}(\xi,t)a(k,\xi,t)\mathrm{e}^{-2\mathrm{i}k\xi} \end{pmatrix}. \tag{3.12}$$

The output $a(k,\ell,t)$ will not differ much from its asymptotic value $a(k,\infty,t)$ if $q(x,t)$ is sufficiently small for $x > \ell$. Consequently, the behaviour of $q(x,t)$ at large x, is essential for (3.5) to deal with real situations adequately. We will see in the next section that it is also crucial for the applicability of the spectral method. We now proceed to show that the numerical solution of the TSRS system (2.2) on a finite interval is in excellent agreement with the theoretical expression for the output (3.5). Note 2

We discretized (2.2) in both x and t using an order 2 Runge–Kutta method and advance via the following algorithm:

(1) given $a(k,x,t)$ and $b(k,x,t)$ for all real k, compute $q(x,t)$ by integrating the time-evolution of q at x for the initial datum $q(x,t=0) = 0$, where the integral is calculated using the trapezoidal rule,

(2) advance to $a(k,x+\mathrm{d}x,t)$ and $b(k,x+\mathrm{d}x,t)$, for all k, by integrating the differential equation for a and b,

(3) go to step 1 with $x = x + \mathrm{d}x$.

The scheme is started at step 1 for $x = 0$.

The quality of the computation is monitored by evaluating the relative error in the total flux $|a(k,x,t)|^2 + |b(k,x,t)|^2$ which is conserved by (2.2). In all the runs that are presented it remained smaller than 10^{-5}.

We chose as parameters

$$\ell = 80, \qquad g = 0.5, \qquad \gamma = 5, \qquad \kappa = 0.2, \tag{3.13}$$

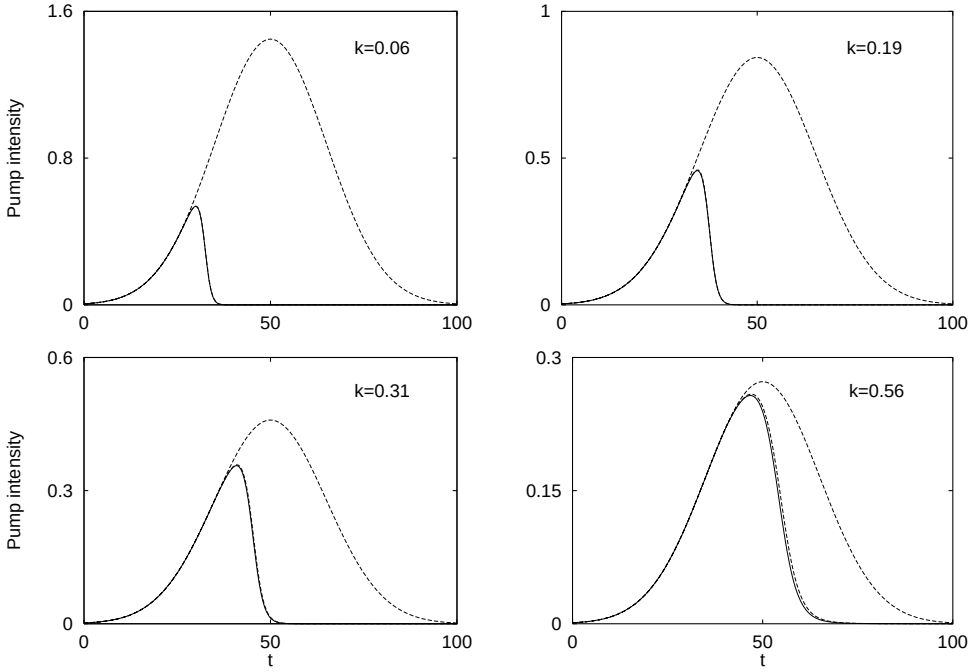

Figure 1. Plots, as functions of time, of the output pump intensity $|a(x = \ell, k, t)|^2$ from the theoretical expression (3.5) (full curves) and the numerical solution of (2.2) (dashed curves) for four different values of k. The large Gaussian curves (dashed curves) represent the input pump intensities $|a(x = 0, k, t)|^2$.

and the input pump pulse envelope is the Gaussian

$$A_0(t) = \exp\left[-\left(\frac{t-50}{30}\right)^2\right]. \tag{3.14}$$

For this choice we found that $\mathrm{d}t \leqslant T/1000$ and $\mathrm{d}x \leqslant \kappa/2$ gave stable results. Another point is that because of the Lorentzian line width we had to take a k interval of width $\approx 80\kappa$ in order to ensure that the integrals were normalized. To describe the strong oscillations present for the zero-GVD system (2.3) we had to choose $\mathrm{d}t \leqslant T/2000$ and $\mathrm{d}x \leqslant \ell/10\,000$.

A typical run with number of grid points in x, t and k ($n_x = n_t = 1000$; $n_k = 500$) takes about 2 h CPU monoprocessor time on an RS10000. We used the parallelism of the problem, i.e. the fact that the marching in x (resp. t) can be made in parallel for the loops in t and k (resp. x) and implemented the code on a Silicon Graphics SGI 10000 using the OpenMP software. This enabled a gain of a factor 8 or 10 in computing time, depending on the number of processors used.

Figure 1 show the pump intensity input $|a(k, 0, t)|^2$ and output $|a(k, \ell, t)|^2$ computed from the IST expression (3.5) together with the numerical solution of the system (2.2) for a length $\ell = 80$ and four different k parameter values, in excellent agreement (a tiny discrepancy is only noticeable in the last plot).

It is worth noting that one cannot pursue a given numerical experiment to a longer length arbitrarily. For instance, we stopped the above calculation at length $\ell = 80$ where the potential $|q(x, t)| < 10^{-5}$. Continuing the run to longer lengths would yield an increase of the potential which would then start to oscillate. This is probably due to the system itself which amplifies

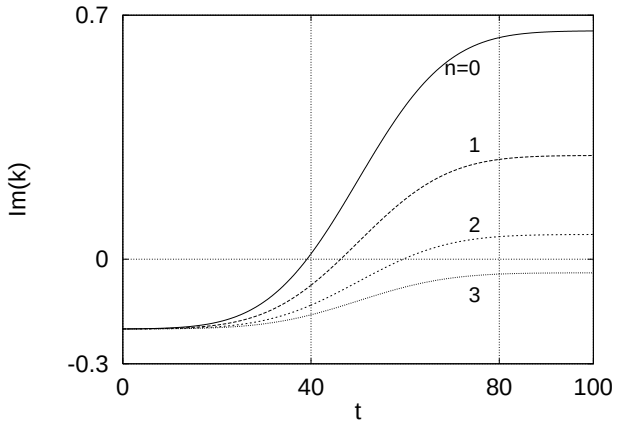

Figure 2. Time evolution of the imaginary part of the poles k_n of ρ for $n = 0, 1, 2$ and 3. The parameters are the same as in figure 1.

the numerical errors in a drastic way at long lengths (note that from the scale invariance (2.8) longer length means larger Raman amplification).

3.4. Raman solitons

The function ρ of (3.10) has an essential singularity in $k = -\mathrm{i}\kappa$ and a set of single poles k_n evolving in time, given by

$$k_n(t) = -\mathrm{i}\kappa + \frac{T(t)}{(n+\frac{1}{2})\pi - \mathrm{i}\gamma}, \tag{3.15}$$

for $n \in \mathbb{N}$. At time zero no pole is present and, as t evolves, poles move upward from $-\mathrm{i}\kappa$ and eventually reach the real axis at the times t_n defined by $\mathrm{Im}\,(k_n(t_n)) = 0$, i.e. by the implicit expression

$$T(t_n) = \frac{\kappa}{\gamma}\left[\gamma^2 + \left[\left(n+\frac{1}{2}\right)\pi\right]^2\right]. \tag{3.16}$$

Note that $t_n = t_{-n-1}$, hence the poles cross the real axis in pairs. The corresponding positions on the real axis are then given by

$$k_n(t_n) = -k_{-n-1}(t_n) = \zeta_n, \qquad \zeta_n = \frac{\kappa}{\gamma}\left(n+\frac{1}{2}\right)\pi. \tag{3.17}$$

In figure 2 we plot the imaginary part of the poles $k_n(t)$ as a function of time for the parameter values (3.13) and $n = 0, 1, 2$ and 3. We observe that the first three poles cross the real axis at the positions $\zeta_0 = 6.310^{-2}$, $\zeta_1 = 0.19$, $\zeta_2 = 0.31$, at times $t_0 = 39.2$, $t_1 = 46.3$ and $t_2 = 59.6$. The pole k_3 starts to evolve with t but cannot cross the real axis because of the finite duration of the pump pulse.

As soon as these poles move to the upper half-plane, they generate a soliton component in the *'potential'* $q(x,t)$. We will prove in the next section that this potential (the medium dynamical variable) is a continuous function of t when a pole crosses the real axis.

3.5. The spectral transform from the output laser pulses

The expressions (3.4) can be inverted to get the following expressions for the Jost solutions in terms of the (physical) fields $a(k,x,t)$ and $b(k,x,t)$ and of the input pulses $A(k,t)$ and

$B(k,t)$:

$$\varphi = \frac{a\overline{A} + \overline{b}B}{|A|^2 + |B|^2}, \qquad \overline{\phi}\mathrm{e}^{2\mathrm{i}kx} = \frac{a\overline{B} - \overline{b}A}{|A|^2 + |B|^2}. \tag{3.18}$$

Then, (3.2) lead to the following formula:

$$\rho(k,t) = \left.\frac{\overline{b}A - a\overline{B}}{a\overline{A} + \overline{b}B}\right|_{x\to\infty} \tag{3.19}$$

which gives the spectral transform $\rho(k,t)$ in terms of the output pump and Stokes fields. This function for k real must become singular at the two points $\pm\zeta_n$ each time a soliton k_n is created and it is used now to prove the generation of Raman solitons in numerical experiments.

For the input pulses given in (2.7) and the particular choice (3.9), from the above we readily obtain

$$\rho = \left.\frac{\overline{b} - a\mathrm{e}^{-\gamma}}{a + \overline{b}\mathrm{e}^{-\gamma}}\right|_{x\to\infty}. \tag{3.20}$$

We use this expression to estimate ρ_ℓ from the numerical solution (a,b) at $x = \ell < +\infty$ and compare it to the ρ obtained from the IST (3.10) for the parameters (3.13). Note that since $|\rho(-k)| = |\rho(k)|$ we will only present positive values of k.

Figure 3 presents the function $|\rho|$ of (3.10) as full curves and the numerical result obtained from (3.20) in $x = \ell$ as dashed curves, for the four values $k = \zeta_0, \zeta_1, \zeta_2$ and ζ_3. Both expressions are very close and as expected $\rho(\zeta_n)$ is singular for $t = t_n$ for $n \leqslant 2$, while it is regular for $n = 3$. In the first panel of figure 3, the dashed curve actually represents the value at $k = 0$, instead of $k = \zeta_0$. This is the only noticeable discrepancy between analytic asymptotic formula and numerical/experimental expression, resulting from the finiteness in x of the data $q(x)$ (the wavelength $\lambda_0 \equiv 2\pi/\zeta_0 \approx 104 > \ell$).

4. Medium

In the previous section we have seen that the finite-length solution is in good agreement with the asymptotic behaviour (3.5) given by the IST on the semi-infinite line. We now proceed to justify this fact by analysing the behaviour of the medium dynamical variable $q(x,t)$.

4.1. Sketch of the inverse problem

IST furnishes the solution $q(x,t)$, called the *medium dynamical variable*, by the expression [15]

$$q(x,t) = 2\mathrm{i}\psi^{(1)}(x,t) \tag{4.1}$$

where $\psi^{(1)}$ is the coefficient of $1/k$ in the Laurent expansion of the function $\psi(k,x,t)$ solution of the following Cauchy–Green coupled system:

$$\begin{aligned}
\varphi(k) &= 1 + \frac{1}{2\mathrm{i}\pi}\int_{-\infty}^{+\infty}\mathrm{d}\lambda\frac{\bar{\rho}(\lambda)\psi(\lambda)}{\lambda - k - \mathrm{i}0}\mathrm{e}^{2\mathrm{i}\lambda x} - \sum_1^N \frac{\bar{\rho}(\bar{k}_n)\psi(\bar{k}_n)}{k - \bar{k}_n}\mathrm{e}^{2\mathrm{i}\bar{k}_n x} \\
\psi(k) &= \frac{1}{2\mathrm{i}\pi}\int_{-\infty}^{+\infty}\mathrm{d}\lambda\frac{\rho(\lambda)\varphi(\lambda)}{\lambda - k + \mathrm{i}0}\mathrm{e}^{-2\mathrm{i}\lambda x} + \sum_{n=1}^N \frac{\rho_n\varphi(k_n)}{k - k_n}\mathrm{e}^{-2\mathrm{i}k_n x}.
\end{aligned} \tag{4.2}$$

Here $\rho_n(t)$ are the N residues of $\rho(k,t)$ at the poles $k_n(t)$ that are in the upper half k-plane (if any). Note that the solution φ corresponds to the solution of (3.1) and that $\psi(k) = \overline{\phi}(\bar{k})$.

Apparently the generation of a soliton is followed by the adjunction of a term in the equation for ψ, and consequently also in the expression of q, leading to a possible discontinuity for q.

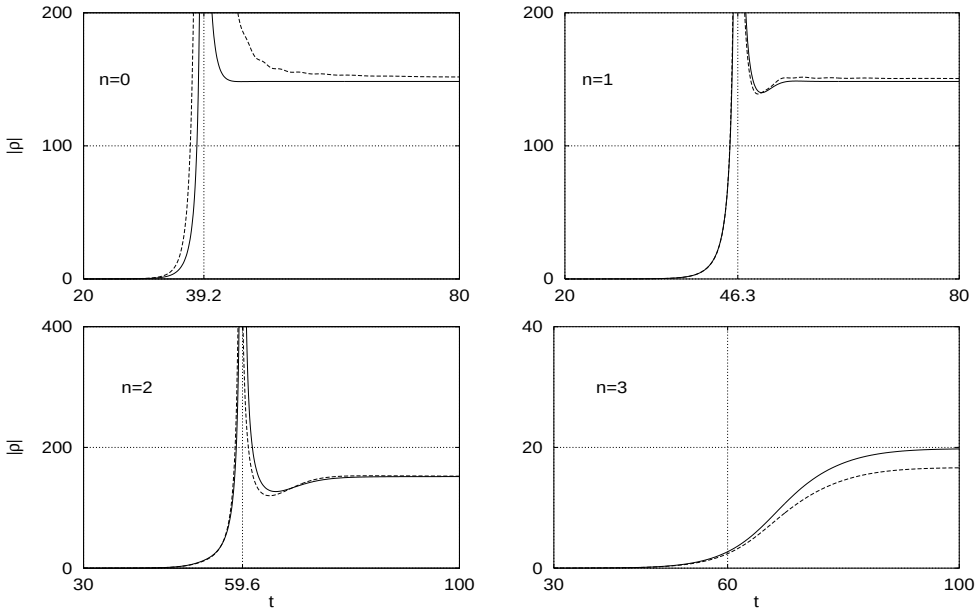

Figure 3. Time evolution of the reflection coefficient $|\rho(\zeta_n)|$ for $n = 0, 1, 2$ and 3 obtained from the inverse scattering theory (3.10) (full curves) and from the numerical solution of (2.2) using formula (3.20) (dashed curves).

We will now proceed to show that this is not the case. This situation is particular to the spectral problem on the semi-line where the continuous spectrum (value of $\rho(k)$ on the real axis) is not separable from the discrete spectrum (poles of ρ in the upper half-complex-plane). This is due to the motion of the poles of ρ that can cross the real axis. In contrast, in the full line case, solitons (discrete spectrum) can exist without radiation (continuous spectrum).

4.2. Continuity

From now on when the spectral parameter k is generically complex we shall denote it by $\boldsymbol{k}$. From what precedes, at $t = t_0$ a pole crosses the real axis at $k = k_0$ from the lower half-plane. We consider here the limits $t \to t_0 \pm 0$, and for $k \in \mathbb{R}$ we write

$$\rho_\pm(k) = \rho(k, t_0 \pm 0) = \frac{R_0(k)}{k - k_0 \mp \mathrm{i}0} \tag{4.3}$$

where $R_0(\boldsymbol{k})$ is analytic in a neighbourhood of k_0. Note that

$$\rho_+(k) = \rho_-(k) + 2\pi\mathrm{i}\rho_0\delta(k - k_0) \tag{4.4}$$

where $\rho_0 = R_0(k_0)$ is the residue of ρ at the pole $k = k_0$.

Assuming for simplicity no other pole, we have from (4.2) at $t = t_0 - 0$

$$\psi(k, x, t_0 - 0) = \frac{1}{2\mathrm{i}\pi}\int_{-\infty}^{+\infty} \mathrm{d}\lambda \frac{\rho_-(\lambda)\varphi(\lambda, x, t_0 - 0)}{\lambda - k + \mathrm{i}0} \mathrm{e}^{-2\mathrm{i}\lambda x} \tag{4.5}$$

which is well defined at $k = k_0$ since the distribution $(\lambda - k_0 + \mathrm{i}0)^{-2}$ is meaningful.

In contrast, at $t = t_0 + 0$, (4.5) diverges due to the distribution $(\lambda - k_0 + \mathrm{i}0)^{-1}(\lambda - k_0 - \mathrm{i}0)^{-1}$. Since there is now a pole in the upper half-complex-plane, we should take the limit $\mathrm{Im}\,(\boldsymbol{k}) \to 0$

in the complete expression in (4.2). i.e.

$$\psi(\boldsymbol{k}, x, t_0 + 0) = \frac{1}{2\mathrm{i}\pi}\int_{-\infty}^{+\infty} \mathrm{d}\lambda \frac{\rho_+(\lambda)\varphi(\lambda, x, t_0 + 0)}{\lambda - \boldsymbol{k}} \mathrm{e}^{-2\mathrm{i}\lambda x} + \frac{\rho_0 \varphi(k_0, x, t_0 + 0)}{\boldsymbol{k} - k_0} \mathrm{e}^{2\mathrm{i}k_0 x}, \tag{4.6}$$

for $\mathrm{Im}\,(\boldsymbol{k}) < 0$. We obtain

$$\psi(k, t_0 - 0) = \psi(k, t_0 + 0). \tag{4.7}$$

and consequently from (4.1)

$$q(t_0 - 0) = q(t_0 + 0). \tag{4.8}$$

4.3. Asymptotic behaviour

We consider here for simplicity the case when solitons are not yet present. Then from (4.1) and (4.2), q can be reconstructed in terms of the reflection coefficient ρ and the Jost solution φ by means of

$$q(x) = -\frac{1}{\pi}\int_{-\infty}^{+\infty} \mathrm{d}k \rho(k)\varphi(k, x)\mathrm{e}^{-2\mathrm{i}kx}. \tag{4.9}$$

This formula directly yields information on the behaviour of q at large x.

In fact, if $\rho(k)\varphi(k, x), \ldots, \partial_k^{(n-1)}\{\rho(k)\varphi(k, x)\}$ are continuous and tend to 0 for $k \to \infty$, and if $\partial_k^{(n)}\{\rho(k)\varphi(k, x)\} \in L(\mathbb{R})$, by repeated integration by parts we obtain

$$q(x) = \left(\frac{\mathrm{i}}{2\pi x}\right)^n \int \mathrm{d}k \partial_k^{(n)}\{\rho(k)\varphi(k, x)\}\mathrm{e}^{-2\mathrm{i}kx}. \tag{4.10}$$

Hence finally,

$$x \to \infty \Rightarrow x^n q(x) \to 0. \tag{4.11}$$

As mentioned in the introduction, such an asymptotic behaviour is not found for the potential $q_0(x, t)$ which would be obtained from TSRS with zero-GVD (2.3). Indeed, in that case the medium initially at rest evolves universally towards the self-similar solution [11] which behaves as $x^{-3/4}$, as found in [12]. More precisely we have

$$q \sim s(t)\xi^{-3/4}[\alpha \cos(h\xi^{1/2} + \beta) + \mathcal{O}(\xi^{-1/2})], \qquad \xi = s(t)x, \tag{4.12}$$

where $s(t)$ is a function of t determined by the boundary conditions and where α, β and h are arbitrary constants.

Figure 4 presents the decay of $|q|$ and $|q_0|$ as dashed and full curves respectively, as a function of x for $t = T/2 = 50$ in a linear-log plot with the parameters given in (3.13). The exponential decay of $|q|$ can be seen for all values of t and follows approximately $\mathrm{e}^{-\kappa x}$, as expected from the analysis. This observation justifies the fact that the finite-length evolution of (2.2) is very close to the asymptotic expression (3.5) given by IST.

In contrast, the slow decay of $|q_0|$ as $x^{-3/4}$ makes it impossible for the integrals of (3.1) to exist so that the scattering theory must be revisited in this case.

4.4. Numerical spectral transform and Raman solitons

By numerical integration of the SRS system (2.2) with a spatial grid of dimension h, we get, at each time value, a set of L discrete data $q(n, t)$ (with $x = nh$ and $\ell = Lh$), that we now analyse by means of the spectral transform. This is easily done, using the results of [16] which, adapted to our notations, reads

$$\rho(k, t) = R_0(\zeta, t), \tag{4.13}$$

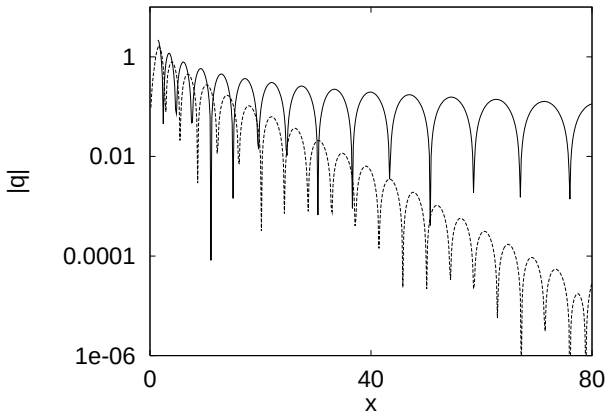

Figure 4. Evolution of $|q|(x, t = 50)$ and $|q_0|(x, t = 50)$ in linear-log coordinates.

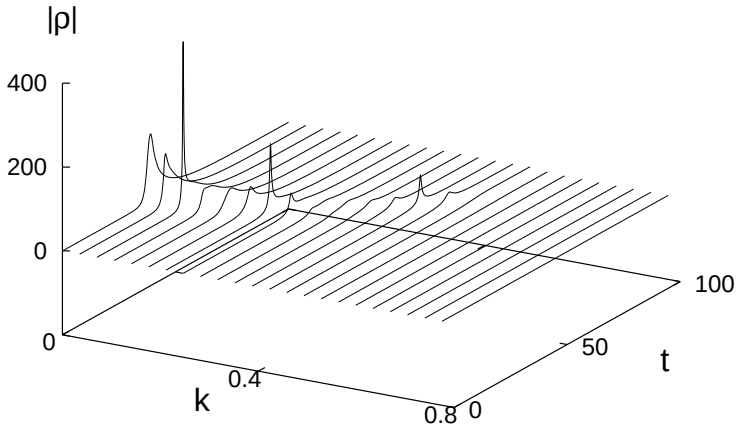

Figure 5. Evolution of $|\rho|(k, t)$ obtained from the discrete spectral transform (4.13).

where R_0 is obtained from the following inverse recursion:

$$R_L = \zeta^L hq(L, t), \qquad R_{m-1} = \frac{R_m - hq(m-1, t)\zeta^{m-1}}{1 + R_m h\bar{q}(m-1, t)\zeta^{-m+1}}, \tag{4.14}$$

and where the parameter ζ is related to k by

$$\zeta = \mathrm{e}^{2\mathrm{i}kh}. \tag{4.15}$$

It is then a simple task to use this recursion relation to compute the numerical spectral transform $R_0(\zeta, t)$ and compare it with the asymptotic theoretical expression (3.10) of $\rho(k, t)$. In figure 5 we plot $|\rho(k, t)|$ where one can clearly see the three singularities (ζ_n, t_n) for $n = 0, 1, 2$ corresponding to the three poles of ρ.

The nonlinear spectral transform is easier to compute, faster and yields more information than the standard Fourier transform which, in particular, does not present any singularity (as we checked numerically).

5. Conclusion

This work demonstrates that the IST solution of transient SRS on the semi-infinite line furnishes a very accurate model for the solution on a finite domain. The accuracy stands not only for the

output laser pulses intensities but also for their phases as shown in a spectacular way by the generation of the Raman solitons. It is shown that the question relating to the experimental observation of Raman solitons is solved by a convenient combination of the output (and input) laser profiles. We also performed a numerical *nonlinear spectral analysis*, which not only proved to be information rich but also quite easy to implement and faster than the usual FFT procedure.

Finally, we mention that it is difficult to compare these results with those obtained in the zero-GVD case (2.3). The problem is that in the limit $\kappa \to 0$, the spectral transform gets an essential singularity in $k = -\mathrm{i}0$ which sends poles to the upper half-plane. To discuss the number and time location of such poles would not only require a careful study of the singular limit $\kappa \to 0$, but also need to reformulate IST on the half-line as we have seen that the potential $q(x)$ does not decrease *quickly enough* as $x \to \infty$.

Acknowledgments

JGC is on leave from the Laboratoire de Mathématiques de l'INSA de Rouen. The authors thank the CRIHAN computing centre for the use of their facilities. We thank INTAS for support through grant 96-339 and support from Sezione INFN di Lecce and PRIN 97 'Sintesi'.

References

[1] Newell A C and Moloney J V 1992 *Nonlinear Optics* (Redwood City, CA: Addison-Wesley)
[2] Yariv A 1975 *Quantum Electronics* (New York: Wiley)
[3] Chu F Y F and Scott A C 1975 *Phys. Rev.* A **12** 2060
[4] Agrawall G P 1989 *Nonlinear Optics* (London: Academic)
[5] Drühl K, Wenzel R G and Carlsten J L 1983 *Phys. Rev. Lett.* **51** 1171
Wenzel R G, Carlsten J L and Drühl K 1985 *J. Stat. Phys.* **39** 621
[6] Claude C and Leon J 1995 *Phys. Rev. Lett.* **74** 3479
Claude C, Ginovart F and Leon J 1995 *Phys. Rev.* A **52** 767
[7] Kaup D J 1983 *Physica* D **6** 143
[8] Steudel H 1990 *Quantum Opt.* **2** 387
[9] Leon J 1992 *Phys. Lett.* A **170** 283
Leon J 1993 *Phys. Rev.* A **47** 3264
Leon J 1994 *J. Math. Phys.* **35** 3054
[10] Gakhovich D E, Grabchikov A S and Orlovich V A 1993 *Opt. Commun.* **102** 485
[11] Fokas A S and Menyuk C R 1999 *J. Nonlinear Sci.* **9** 1
[12] Menyuk C R, Levi D and Winternitz P 1992 *Phys. Rev. Lett.* **69** 3048
Levi D, Menyuk C R and Winternitz P 1991 *Phys. Rev.* A **44** 6057
[13] Menyuk C R 1993 *Phys. Rev.* A **47** 2235
[14] Levi D, Menyuk C R and Winternitz P (ed) 1994 *Self-Similarity in Stimulated Raman Scattering* (Montreal: Les Publications CRM)
[15] Leon J and Mikhailov A V 1999 *Phys. Lett.* A **253** 33
[16] Boiti M, Leon J and Pempinelli F 1996 *Phys. Rev.* E **54** 5739
Boiti M and Pempinelli F 1997 *Inverse Problems* **13** 919

Author queries

Note 1 (Page 3):
Sense as intended?

Note 2 (Page 5):
Sense as intended?